Chapter 2
Metal-Modified Carbide Anode Electrocatalysts

Zachary J. Mellinger and Jingguang G. Chen

Abstract Fuel cells are being extensively studied to help ease the potential energy crisis. There have been many recent advances in direct methanol fuel cells (DMFC). These devices have shown promise for portable power applications because of the high gravimetric energy density of methanol. One major limitation of the technology is its extensive use of platinum in its anode catalyst. This chapter will provide a review of the work done to eliminate or significantly decrease the amount of platinum in DMFC catalysts by replacing platinum with tungsten monocarbide (WC) and monolayer coverages of platinum or palladium on WC.

2.1 Introduction

While there has been much progress in DMFC technology, there are still technical hurdles that remain for large-scale commercialization. One of the challenges with the anode electrocatalyst is the high cost and low abundance of the leading catalyst materials: Pt and Ru. Another challenge is the strong binding of CO molecules to Pt and Ru, which leads to CO poisoning of the active sites and slow kinetics for the electrooxidation of methanol [1]. The commercialization of DMFC depends upon new catalytic materials being developed that are more cost-effective and show a higher CO tolerance. This can be achieved by either finding a new catalyst or modifying the current catalysts.

A potential alternative electrocatalyst is tungsten carbide, which has attracted attention from researchers since Levy and Boudart discovered that tungsten carbides had similar catalytic behavior to Pt [2]. The Levy and Boudart study has led to many groups researching tungsten carbides as alternatives to Pt for

Z.J. Mellinger • J.G. Chen (✉)
Department of Chemical Engineering, University of Delaware, Newark, DE 19716, USA
e-mail: jgchen@UDel.Edu

M. Shao (ed.), *Electrocatalysis in Fuel Cells*, Lecture Notes in Energy 9,
DOI 10.1007/978-1-4471-4911-8_2,

catalytic and electrocatalytic applications [3–5]. Some of the initial studies focused on single-crystal surfaces in an ultrahigh vacuum (UHV) environment [6–11] and density functional theory (DFT) calculations [12]. Studies were also being performed using Pt- and Pd-modified tungsten carbides. Replacing Pt with Pd is desirable as Pd is cheaper and more abundant than Pt as is discussed in one of the chapters. Pt- and Pd-modified tungsten carbides are also promising potential electrocatalysts because having an electrocatalytically active support decreases the precious metal loading needed while possibly adding a synergistic effect between the materials.

Our research group attempted to bridge the "materials gap" and "pressure gap" between fundamental surface science studies and industrially applicable catalysts. This bridging was needed because while single-crystal and UHV studies have provided fundamental insights into the catalytic behavior of tungsten carbides and metal-modified tungsten carbides, an industrially applicable catalyst would have the form of carbide catalysts on large surface area supports. Our group first investigated the reaction pathways of methanol on single-crystal surfaces of tungsten carbide and Pt-modified tungsten carbide [6–11]. Then those single-crystal results were extended to the synthesis, characterization, and electrochemical evaluation of polycrystalline tungsten carbide and metal-modified tungsten carbide films [11, 13–22]. Electrochemical studies were performed in acid as well as basic solutions as pH and type of solution affect the performance of electrocatalysts. Finally, supported particles of tungsten carbide and Pt-modified tungsten carbide were tested in full-cell measurements [23]. These studies bridged the "materials gap" and "pressure gap" between DFT and UHV studies on model surfaces and the evaluation of relevant supported electrocatalysts throughout the literature [23–30].

2.2 Theoretical and Experimental Studies on Single-Crystal Surfaces

2.2.1 DFT Studies

DFT studies of single-crystal and polycrystalline surfaces have provided a fundamental understanding of the reaction pathways of methanol decomposition on tungsten carbide and metal-modified tungsten carbide surfaces. The binding energies of methanol and methoxy species are shown in Table 2.1 on different surfaces [14, 16, 31, 32]. For both methanol and methoxy, tungsten carbide showed the highest binding energy, and adding a monolayer of Pt or Pd decreased the binding energy closer to that of the pure metals. The methanol and methoxy binding energies are similar to the literature for Pd(111) [33–36] and Pt(111) [37, 38]. The trend in Table 2.1 predicts that metal-modified WC surfaces should show activity more similar to the parent metals than to tungsten carbide. Additionally, metal-modified

Table 2.1 Binding energies of methanol and methoxy on metals, tungsten carbide, and metal-modified tungsten carbide surfaces

	Binding energy (kcal/mol)				
	Methanol	Methoxy			
	Binding site				
	Atop	Atop	fcc	hcp	Bridge
Pt(111) [32]	−4.50	−31.80			
Pd(111) [14]	−5.56	−33.79	−38.00	−37.69	−37.22
WC(0001) [16]	−19.07		−51.16		
Pt/WC(0001) [16]	−8.37		−5.35		
Pt [31]	−4.86	−34.91	−32.95	−31.33	−31.93
WC [14, 31]	−15.86	−66.38	−81.94	−91.09	−73.95
Pt/WC [31]	−10.59	−49.49	ns	−48.97	−48.9
Pd/WC [14]	−8.58	−48.62	−55.33	−54.84	−52.25

ns not stable

tungsten carbide surfaces should show higher total activity than parent metals because of the higher methanol and methoxy binding energies. These DFT studies provided the basis for selecting relevant model surfaces for UHV experiments.

2.2.2 TPD Studies on Single-Crystal Surfaces

For the UHV experiments, surface preparation and characterization of C/W(111) have been described in detail previously [8]. Clean W(111) was dosed with ethylene at 120 K and then annealed to 1,200 K, producing C/W(111). The Pt/C/W(111) surface was synthesized by depositing Pt by evaporative deposition by resistively heating a W wire which was wrapped with Pt wire [10]. Previous studies using Auger electron spectroscopy (AES) had determined that Pt grows on tungsten carbide through a layer-by-layer mechanism [39, 40]. This growth mechanism means that submonolayer coverages of Pt form regions of monolayers on the tungsten carbide surfaces, as opposed to forming nanoparticles. Thus, Pt could be deposited onto the carbide surface with precise control over the surface coverage. Temperature-programmed desorption (TPD) and high-resolution electron energy loss spectroscopy (HREELS) were used to determine the decomposition pathways of methanol on Pt (111) [17, 41], C/W(111) [16, 17], Pt/C/W(111) [16, 17], C/W(110) [11], Pt/C/W (110) [11], and Pd(111) [14, 42, 43]. Methanol has been found to decompose via the following net reaction pathways under UHV conditions:

$$aCH_3OH \rightarrow aC_{ad} + aO_{ad} + 2aH_2 \quad \text{(complete decomposition)} \tag{2.1}$$

$$bCH_3OH \rightarrow bCO + 2bH_2 \quad \text{(reforming, desired reaction)} \tag{2.2}$$

$$cCH_3OH \rightarrow cCH_4 + cO_{ad} \quad \text{(methane production)} \tag{2.3}$$

Table 2.2 Activity of methanol decomposition on single-crystal surfaces of metals, tungsten carbides, and metal-modified tungsten carbides

Methanol activity (ML)				
Surface	Reforming	Decomposition	CH_4	Total
Pt(111) [41]	~0	~0	~0	~0
Pd(111) [14]	0.079[a]	0.000[a]	0	0.079[a]
C/W(111) [9]	0.087	0.155	0.038	0.28
0.6 ML Pt/C/W(111) [10]	0.091	0.086	0	0.177
C/W(110) [6]	0.06	0.176	0.068	0.304
0.5 ML Pt/C/W(110) [11]	0.049	0.174	0	0.223

[a][42]

where *a*, *b*, and *c* denote the amount of methanol molecules undergoing each pathway. The reforming pathway is the desired reaction as this extracts the most hydrogen from the fuel while not coking up the catalyst surface. The CO product can be further reacted on the surface to produce CO_2 to release two more electrons. The production of CO in the reforming reaction pathway is the reason why CO tolerance is an important characteristic of an anode DMFC catalyst. Also, the removal of the methane production pathway is critical for the efficient utilization of methanol because it leads to losing four of the six electrons available from the methanol electrooxidation reaction.

The quantification of the TPD results for the reactions of methanol on various single-crystal surfaces is shown in Table 2.2. The methods used to quantify the TPD results are described in the literature [44]. These results indicate that there is a synergistic effect by supporting submonolayer coverage Pt on WC(111) and WC(110); the Pt-modified WC single-crystal surfaces still had a high activity for methanol decomposition while eliminating the production of the undesirable methane production pathway. The selectivity toward the reforming reaction pathway was higher for the Pt-modified surfaces when compared to the metal single crystals.

2.2.3 Vibrational Studies of Single-Crystal Surfaces

To further characterize the intermediates on the surfaces, vibrational studies using HREELS were performed with methanol dosed between 90 and 100 K on the single-crystal surfaces. The results of the HREELS experiments are summarized in Table 2.3. The HREELS spectra of methanol on various surfaces include an O–H stretching mode at ~3,200 cm^{-1}, a symmetric and asymmetric C–H stretching modes at ~3,000 cm^{-1}, CH_3 deformation features at ~1,475 cm^{-1}, a CH_3 rocking mode at ~1,150 cm^{-1}, a CO stretch at ~1,000 cm^{-1}, an O–H deformation at ~700 cm^{-1}, and a metal-O stretch at ~400 cm^{-1}. The spectra on the carbon-modified tungsten surfaces showed that the methanol adsorbed as methoxy, indicative that the tungsten carbide surfaces adsorbed methanol dissociatively breaking the O–H bond. The Pt-modified surfaces still showed a weak O–H stretching mode at around 3,200 cm^{-1}

Table 2.3 HREELS assignments for methanol on single-crystal surfaces (in cm^{-1})

Mode	Gas phase	Liquid phase[a]	Pt (111)[c]	Pd (111)[d]	C/W (111)[e]	0.6 ML Pt/C/W (111)[f]	C/W (110)[g]	0.5 ML Pt/C/W (110)[g]
ν(OH)			3,220			3,470		
$\nu_{as}(CH_3)$	3,000	2,980	2,930	3,015	2,956	2,976	2,936	2,963
	2,960[a]	2,946		2,865			2,821	
ν(M–CO)								
$\delta(CH_3)$	1,455;	1,480	1,410	1,430	1,454	1,454	1,448	1,461
	1,477[a]			1,375				
$\rho(CH_3)$	1,124[b]			1,140	1,157	1,150	1,157	1,150
ν(CO)	1,033[a]	1,030	970	1,005	1,035	1,028	1,028	1,025
δ(OH)			680					
ν(M–O)				325		670		

[a][32]
[b][62]
[c][41]
[d][43]
[e][8]
[f][10]
[g][11]

which indicated that at least some of the methanol adsorbed molecularly on those surfaces. This was confirmed as the spectrum of Pt(111) showed a strong O–H stretching feature as nearly all the methanol adsorbed molecularly [41]. In contrast, Pd(111), which will be further examined later, adsorbed methanol as a methoxy intermediate [43].

As the surfaces were heated, the intermediates that were left adsorbed to the surfaces were investigated for the different single-crystal surfaces. For the C/W (111) and C/W(110) surfaces, the methoxy was found to react without producing any other surface intermediates. The Pt-modified surfaces reacted at a lower temperature than the pure carbides. The methanol on Pt(111) mostly desorbed from the surface by 300 K [41]. These conclusions from the single-crystal studies were then applied to study polycrystalline foils which are much more realistic surfaces than the idealized single crystals.

2.3 Surface Science and Half-Cell Measurements on Polycrystalline Surfaces

Studies of the clean and Pt-modified carburized W single crystals provided a fundamental understanding of how methanol decomposition proceeds under UHV conditions. These studies suggest that tungsten carbide-based electrocatalysts, especially metal-modified tungsten carbides, are promising anode catalyst materials to replace Pt in the DMFC. These conclusions are further examined on more applicable polycrystalline foils. These foils are better representations of the complex morphology

of real catalysts. These materials also can be more easily used to electrochemically evaluate the catalysts. In these experiments, chronoamperometry (CA), cyclic voltammetry (CV), X-ray photoelectron spectroscopy (XPS), TPD, and HREELS have been used to analyze the activity and selectivity of these polycrystalline films toward the electrooxidation of methanol. These samples were synthesized by either carburizing a polycrystalline tungsten foil [14] or by depositing WC on a carbon substrate [19, 22]. These different WC thin films were characterized by a combination of various techniques including X-ray diffraction (XRD), AES, and XPS. The samples were found to be phase-pure WC in the bulk as well as on the surface. The Pt- and Pd-modified surfaces were synthesized either by evaporative deposition [14] or incipient wetness impregnation [45] and were characterized by AES and XPS. Pd has been found to follow a layer-by-layer growth mechanism on WC [14]. Electrochemical studies were performed as described previously [14, 20].

2.3.1 TPD Studies of Methanol on Polycrystalline Surfaces

The TPD quantification results of methanol on WC and metal-modified WC are summarized in Table 2.4. These results show that modifying the polycrystalline WC foil with Pt takes away the methane production pathway. The 0.5 ML Pt/WC surface had a higher selectivity toward the reforming reaction and a much higher activity than the pure Pt foil. The 1 ML Pt/WC surface also had a higher activity than Pt foil but with a lower selectivity toward the reforming reaction. For the Pd-modified WC surfaces, even a low Pd loading such as 0.5 ML Pd significantly reduced the methane production pathway, while it was completely removed with 1 ML Pd. While not having as high of a selectivity toward reforming as Pd(111), there was a much greater overall and reforming activity for the 0.5 ML Pd/WC surface. The 1 ML Pd/WC surface also had a higher reforming activity than Pd(111). Another property that was examined for these polycrystalline surfaces through TPD was the CO tolerance. The CO TPD results of CO dosed on to Pd(111), Pt, tungsten monocarbide (WC), Pt/WC, and Pd/WC surfaces are compared in Fig. 2.1 [14, 15]. These results show that supporting the Pt and Pd with WC decreased the CO desorption temperature, suggesting an increase in the CO tolerance of the catalysts. Another property that increased CO tolerance was the ability for a surface to dissociate water. Tungsten carbides and Pt-modified tungsten carbides are more active toward water dissociation than Pt(111) [11].

2.3.2 Vibrational Studies of Polycrystalline Surfaces

HREELS measurements were performed to further examine the reaction pathways of methanol that were observed on the polycrystalline WC and metal-modified WC surfaces. Table 2.5 shows the HREELS vibrational features of the polycrystalline

Table 2.4 Activity of methanol decomposition on polycrystalline surfaces of metals, tungsten carbides, and metal-modified tungsten carbides

Methanol activity (ML)				
Surface	Reforming	Decomposition	CH_4	Total
Pt [16]	0.006	0.04	0	0.046
WC [14, 16]	0.02	0.182	0.023	0.225
0.5 ML Pt/WC [16]	0.018	0.107	0	0.125
1 ML Pt/WC [16]	0.006	0.079	0	0.085
0.5 ML Pd/WC [14]	0.183	0.083	0.011	0.277
1 ML Pd/WC[14]	0.053	0.152	0	0.205

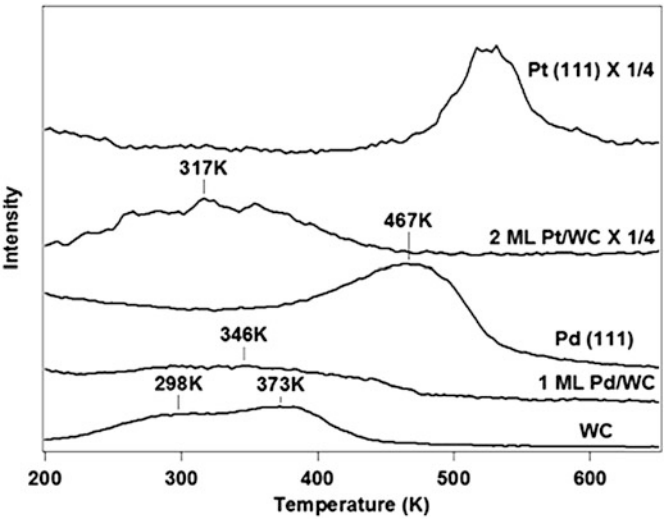

Fig. 2.1 CO TPD on Pt(111), 2 ML Pt/WC, Pd(111), 1 ML Pd/WC, and WC following adsorption of CO at 100 K

Table 2.5 HREELS assignments for methanol on polycrystalline surfaces (in cm^{-1})

Mode	Gas phase	Liquid phase[a]	Pt[c]	WC[d]	0.5 ML Pt/WC[c]	1 ML Pd/WC[d]
ν(OH)			3,626		3,606	3,301
$\nu_{as}(CH_3)$	3,000; 2,960[a]	2,980; 2,946	2,970; 3,369	2,936	2,929; 3,277	2,936
ν(M-CO)			1,860; 2,036	2,043	2,036	2,043
δ(CH3)	1,455; 1,477[a]	1,480	1,454	1,441	1,444	1,448
ρ(CH3)	1,124[b]		1,150	1,150	1,136	1,143
ν(CO)	1,033[a]	1,030[c]	1,021	1,015	1,021	1,028
δ(OH)					717	737

[a][32]
[b][62]
[c][16]
[d][14]

surfaces following methanol adsorption. Similar to the single-crystal surfaces, WC was found to adsorb methanol as a methoxy intermediate. When the WC surface was heated up to ~350 K, the C–O bond was broken which confirmed what the TPD results showed with the presence of the methane production pathway [14, 16]. The polycrystalline Pt surface showed that the adsorbed molecular methanol reacted through an aldehyde intermediate. Above 300 K, the Pt surface showed an increase in the aldehyde feature as well as a C–O stretching peak [16]. The Pt-modified WC surfaces also showed that the methanol reacted through the aldehyde intermediate; however, with this surface, the C–H bond broke before the C–O bond [16]. The Pt-modified WC showed that the origin of the synergistic effect of supporting Pt on WC can be attributed to the different chemical properties of the modified surface [17]. For the Pd-modified WC surfaces, there was a weak O–H stretching mode. There was no η^2-formaldehyde intermediate as was seen on the Pd(111) surface [43]. The methoxy on Pd-modified WC reacted at a lower temperature than on the WC surface [14]. The reaction temperature for methoxy on Pd/WC [14] was lower than that of Pt/WC [16], Au/WC [31], and Ni/WC [31] and was similar to Rh/WC [31]. Overall, the metal-modified catalysts decomposed methoxy at a lower temperature with a greater selectivity toward the reforming reaction pathway. The metal-modified surfaces also showed an increased CO tolerance when compared with the parent metals. These surface science experiments were then extended to electrochemical testing of the activity, selectivity, and stability of the surfaces.

2.3.3 Electrochemical Evaluation of Polycrystalline WC and Metal-Modified WC

2.3.3.1 CO Stripping Experiments

The surface science studies of both single-crystal and polycrystalline surfaces suggest that WC and metal-modified WC are promising DMFC anode electrocatalysts. The next step is to bridge the "pressure gap" and test the polycrystalline catalysts in atmospheric pressure. The first set of experiments examined the CO tolerance of the polycrystalline catalysts in an electrochemical environment through CO stripping voltammetry as described earlier [15]. Pt foil, Pt supported on carbon paper, WC on carbon paper, and Pt-modified WC on carbon paper were exposed to CO followed by two consecutive cyclic voltammograms. The first scan stripped off the CO, showing at what potential CO was oxidized and removed from the sample. The second scan provided a clean scan of the surface from which to compare the first "poisoned" scan. For Pt foil and Pt supported on carbon paper, the results were similar with CO stripping peaks at ~0.75 V (all potentials are recorded versus the normal hydrogen electrode) in a 0.05 M solution of H_2SO_4. For the sample of WC supported on carbon paper, a broad peak at ~0.45 V was observed. For the Pt-modified WC on carbon paper, there was a peak at ~0.75 V as well the start of CO oxidation as low as ~0.28 V.

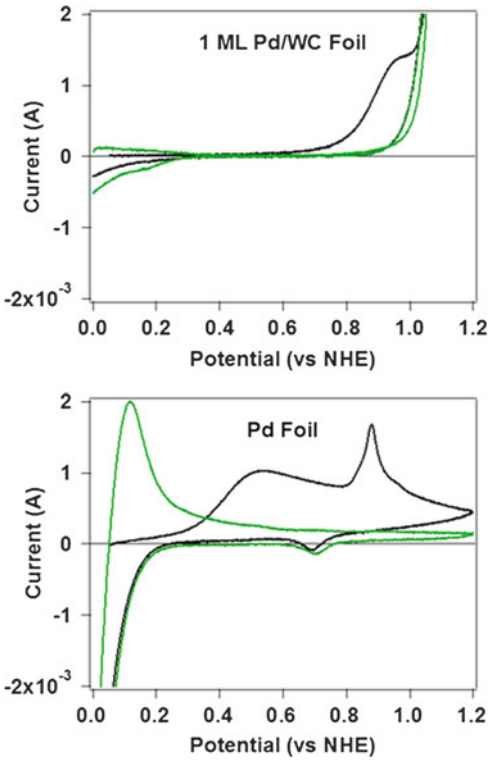

Fig. 2.2 CO stripping voltammetry on 1 ML Pd/WC foil and Pd foil

These results confirmed that using WC as a substrate increases the CO tolerance of the Pt catalyst [15].

This same procedure was performed for a Pd foil and 1 ML Pd/WC in a 0.05 M H_2SO_4 environment. The results of this CO stripping voltammetry are shown in Fig. 2.2. The two peaks on the Pd foil CO stripping scan show the CO being oxidized from the steps (~0.55 V) and terraces (~0.88 V) of the foil [46]. For the 1 ML Pd/WC surface, the oxidation peak starts below the potential at which the Pd foil terrace sites start to oxidize CO. This figure also suggests that using WC as a substrate increases the CO tolerance of the precious metal.

2.3.3.2 Methanol Electrooxidation on WC and Metal-Modified WC in Acidic and Alkaline Media

CV and CA experiments were performed to examine the electrochemical activity of Pt, Pd, WC, Pt/WC, and Pd/WC activity toward methanol electrooxidation. Experiments were performed with Pt, 0.8 ML Pt/WC, and WC samples in a 0.2 M CH_3OH and 0.05 M H_2SO_4 electrochemical environment [20]. The Pt foil showed methanol oxidation peaks at ~0.9 V on the forward scan at ~0.7 V on the

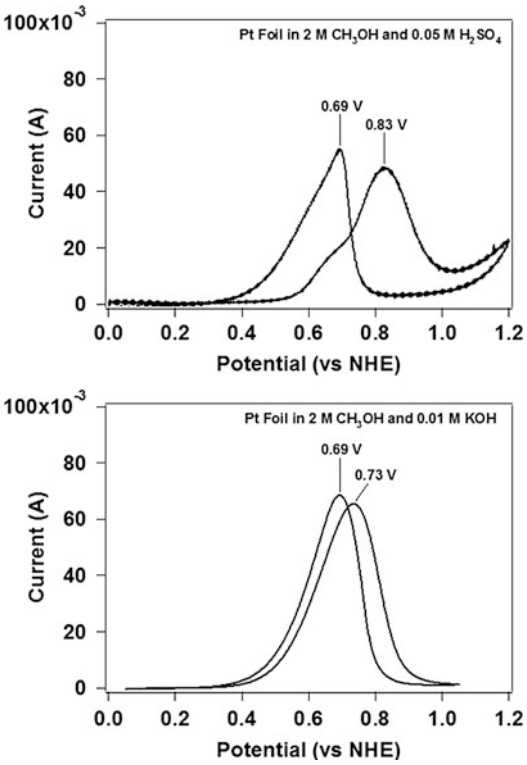

Fig. 2.3 Methanol CV of Pt foil in acidic and alkaline environments

reverse scan. The WC surface exhibited a methanol oxidation peak at ~0.65 V on the forward scan and no features on the reverse scan. The 0.8 ML Pt/WC surface showed similar features to the WC surface but with greater stability of the curves. CA was also performed on the three surfaces at a potential of 0.65 V. These results showed that the WC and 0.8 ML Pt/WC surfaces had a significantly higher steady state current than the Pt foil [20]. The higher steady state current for WC and 0.8 ML Pt/WC can be at least partially explained by the higher CO tolerance.

Experiments were performed with Pd, WC, and 1 ML Pd/WC surfaces in a 2 M CH_3OH and 0.01 M KOH environment [14]. An alkaline solution was chosen for the palladium experiments as Pd-based catalysts in this environment have been shown to have a higher CO tolerance and an increased activity for methanol oxidation when compared to Pt-based catalysts [29, 47–50]. As a means of comparison between acidic and alkaline CV, Pt foil samples were tested using CV in a 0.01 M KOH as well as a 0.05 M H_2SO_4 solution, both with 2 M CH_3OH. The results are shown in Fig. 2.3 with both of the spectra having peaks on the forward and reverse scans but at different potentials. The Pt foil in the alkaline environment shows slightly higher currents. The Pd foil surface shows a methanol oxidation peak at 0.86 V on the forward scan and 0.77 V on the reverse scan. The WC CV experiments in alkaline media showed no activity toward methanol oxidation. The 1 ML Pd/WC foil showed similar methanol

oxidation activity as Pd foil with oxidation peaks at 0.89 V on the forward scan and 0.71 V on the reverse scan. The CA experiments showed that the 1 ML Pd/WC surface had a higher steady state activity and maintained a higher stability over a 2-h scan when compared to Pd foil [14]. Again, this higher steady state activity and stability can be at least partially explained by the higher CO tolerance of the 1 ML Pd/WC surface.

2.3.3.3 Electrochemical Stability of WC and Metal-Modified WC

Surface stability in an electrochemical environment is one of the critical requirements in developing an effective electrocatalyst. XPS measurements were performed before and after the electrochemical experiments to directly probe the oxidation state of the surface metal atoms. Some of these experiments were performed with a setup that allowed the surface to be kept in a UHV environment between experiments as described previously [18, 20]. XPS experiments investigate whether a surface is irreversibly oxidized or dissolved from the surface during the electrochemical experiments. For all the experiments on WC and metal-modified WC, phase-pure WC was confirmed before experiments were performed. It was found that for CV of clean WC, the surface could be ramped up to ~0.8 V for 30 cycles in a 0.05 M H_2SO_4 environment without showing surface oxidation [18]. Pt deposited on WC was found to help protect the WC from forming surface oxides, even when ramped up to a potential of 1.2 V. In these experiments, the Pt loading was not found to decrease after the CV experiments [15]. These experiments confirmed that there is a synergistic effect for the Pt/WC surface with the samples showing a higher CO tolerance than Pt and with greater stability and activity than WC [15]. For the alkaline environment experiments, there was little oxidation on the surface after the 2-h CA experiments on the WC and 1 ML Pd/WC surfaces. With the 1 ML Pd/WC surface, there was a 20 % loss in Pd on the surface after the 2-h experiment. This loss was either due to agglomeration or dissolution of the Pd metal. The electrochemical experiments on Pt-modified WC were then expanded to full-cell testing of WC and Pt/WC nanoparticles.

2.4 Full-Cell Measurements of Supported Catalysts

Supported nanoparticles are the main catalysts used in current fuel cell devices. The combined DFT, single crystal, polycrystalline, and electrochemical experiments demonstrated that WC and Pt/WC have catalytic properties that are promising for use as anode DMFC electrocatalysts. These fundamental results still left questions unanswered as to how these materials could be incorporated into a realistic device. These questions led to studies of WC and Pt/WC nanoparticles in a fuel cell test station [23]. The WC nanoparticles were obtained from Japan New Metals Company. The Pt/WC nanoparticles were prepared with a 10 wt% Pt loading using incipient

wetness impregnation [45]. In preparing the membrane electrode assembly (MEA), the nanoparticles were coated on a Nafion 117 membrane. This combination was then hot pressed along with the gas diffusion layer into the MEA, which was then evaluated using an Arbin Instruments fuel cell test stand [23].

2.4.1 Characterization of WC Nanoparticles

The WC nanoparticles were characterized using XRD, XPS, and scanning electron microscopy (SEM). XRD and XPS were used to confirm that the nanoparticles were phase-pure WC in the bulk and on the surface, respectively. SEM was then used to confirm the WC particle size. The XPS results also revealed that ~25 % of the tungsten signal for the WC nanoparticles were due to tungsten oxides and that there was some carbonaceous carbon on the surface. After the synthesis of the Pt/WC nanoparticles, the amount of the tungsten signal that was now tungsten oxides increased to ~50 % [23].

2.4.2 Fuel Cell Evaluation of WC and Pt/WC Nanoparticle Anode Electrocatalysts

Power density and polarization curves for the Pt/WC nanoparticles are shown in Fig. 2.4 [23] with a summary of the data in Table 2.6 [23]. These curves were generated by withdrawing specific current density values for 5-min intervals. The output of the MEA was monitored within the normal temperature ranges for DMFC evaluation [51–54]: 323 K, 333 K, and 343 K. As the temperature increased, so did the MEA performance, suggesting that the reaction was kinetically limited. With the increase in temperature from 323 K to 343 K, the power density of the MEA was increased from 6.8 mW/cm^2 to 14.5 mW/cm^2. The open-circuit voltage for the Pt/WC nanoparticles also increased with temperature going from 460 mV at 323 K to 500 mV at 343 K. On Pt/WC, the electrooxidation of methanol was found to be reaction limited as the position of the maximum power density was within the linear region of the polarization curve. Also, the polarization curves lack of a mass transfer limited regime suggested that the cell performance was likely limited by the surface area of the anode electrocatalyst. The Pt/WC nanoparticle MEA was also compared to an MEA with a Pt/Ru anode electrocatalyst. The results in Table 2.6 show that, on the basis of power per mg of metal loading, the Pt/WC MEA delivered about the same power as the Pt/Ru MEA. The MEAs for the WC and Pt/WC catalysts were not optimized, leaving the possibility for significant improvement. These results showed that as a realistic catalyst in a full-cell test station, Pt/WC showed promise as an alternative DMFC electrocatalyst to Pt and Pt/Ru catalysts.

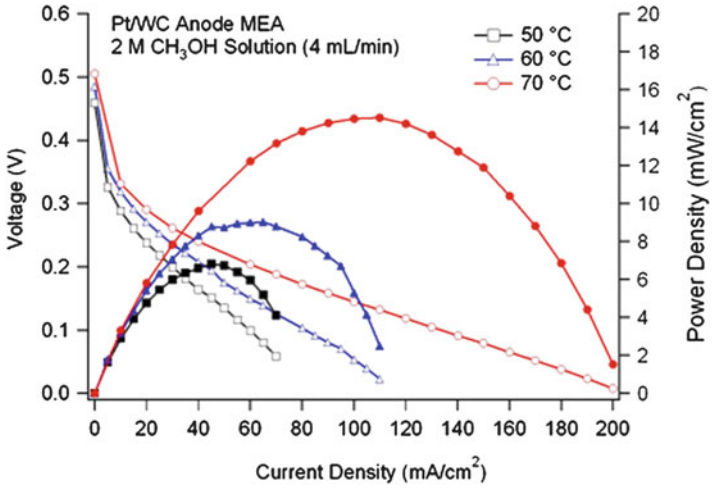

Fig. 2.4 Power density and polarization curves of a Pt/WC anode MEA with a 2 M methanol concentration and a flow rate of 4 ml/min at various operating temperatures [23]

Table 2.6 Maximum power density and cell voltage values at various temperatures for Pt/WC and Pt/Ru anode MEAs

	Anode MEA (2 M CH_3OH, 4 ml/min)		
	Temperature (K)	Power density (mW/cm^2)	Power per mg Pt at anode (mW/mg Pt)
Pt/WC nanoparticles	323	6.8	17.0
	333	9.1	22.8
	343	14.5	36.3
Pt/Ru nanoparticles	323	67.5	16.9
	333	98.4	24.6
	343	120.1	30.0

2.5 Conclusions

This chapter describes the research approach of combining DFT, UHV surface science studies, half-cell electrochemical evaluation, and full-cell testing to identify DMFC electrocatalysts with desirable properties. These different studies bridged both the "materials gap" and "pressure gap" by applying the fundamental understanding gained from theoretical and surface science studies to industrially relevant supported nanoparticle electrocatalysts. For the purpose of finding anode electrocatalysts for DMFC, this approach illustrates the potential to substitute WC-supported Pt or Pd for the Pt/Ru anode electrocatalyst. These results also suggest WC, Pt/WC, and Pd/WC are active and stable electrocatalysts which can be explored for other electrocatalytic applications [13, 39, 55–61].

References

1. Liu H, Song C, Zhang L, Zhang J, Wang H, Wilkinson DP (2006) A review of anode catalysis in the direct methanol fuel cell. J Power Sources 155:95–110
2. Levy RB, Boudart M (1973) Platinum-like behavior of tungsten carbide in surface catalysis. Science 181(4099):547–549
3. Chen JG (1996) Carbide and nitride overlayers on early transition metal surfaces: preparation, characterization, and reactivities. Chem Rev 96:1477–1498
4. Hwu HH, Chen JG (2005) Surface chemistry of transition metal carbides. Chem Rev 105: 185–212
5. Oyama ST (1996) The chemistry of transition metal carbides and nitrides. Blackie Academic and Professional, London
6. Hwu HH, Chen JG (2003) Potential application of tungsten carbides as electrocatalysts: 4. Reactions of methanol, water, and carbon monoxide over carbide-modified W(110). J Phys Chem B 107:2029–2039
7. Hwu HH, Chen JG (2003) Potential application of tungsten carbides as electrocatalysts. J Vac Sci Technol A 21:1488–1493
8. Hwu HH, Chen JG, Kourtakis K, Lavin JG (2001) Potential application of tungsten carbides as electrocatalysts. 1. Decomposition of methanol over carbide-modified W(111). J Phys Chem B 105:10037–10044
9. Hwu HH, Polizzotti BD, Chen JG (2001) Potential application of tungsten carbides as electrocatalysts. 2. Coadsorption of CO and H_2O on carbide-modified W(111). J Phys Chem B 105:10045–10053
10. Liu N, Kourtakis K, Figueroa JC, Chen JG (2003) Potential application of tungsten carbides as electrocatalysts: III. Reactions of methanol, water, and hydrogen on Pt-modified C/W(111) surfaces. J Catal 215:254–263
11. Zellner MB, Chen JG (2005) Potential Application of tungsten carbides as electrocatalysts: synergistic effect by supporting Pt on C/W(110) for the reactions of methanol, water, and CO. J Electrochem Soc 152:A1483–A1494
12. Kitchin JR, Nørskov JK, Barteau MA, Chen JG (2005) Trends in the chemical properties of early transition metal carbide surfaces: A density functional study. Catal Today 105:66–73
13. Esposito DV, Chen JG (2011) Monolayer platinum supported on tungsten carbides as low-cost electrocatalysts: opportunities and limitations. Energy Environ Sci 4:3900–3912
14. Mellinger ZJ, Kelly TG, Chen JG (2012) Pd-modified tungsten carbide for methanol electro-oxidation: from surface science studies to electrochemical evaluation. ACS Catal 2:751–758
15. Mellinger ZJ, Weigert EC, Stottlemyer AL, Chen JG (2008) Enhancing CO tolerance of electrocatalysts: electro-oxidation of CO on WC and Pt-modified WC. Electrochem Solid-State Lett 11(5):B63–B67
16. Stottlemyer AL, Liu P, Chen JG (2010) Comparison of bond scission sequence of methanol on tungsten monocarbide and Pt-modified tungsten monocarbide. J Chem Phys 133:104702
17. Stottlemyer AL, Weigert EC, Chen JG (2011) Tungsten carbides as alternative electrocatalysts: from surface science studies to fuel cell evaluation. Ind Eng Chem Res 50: 16–22
18. Weigert EC, Esposito DV, Chen JG (2009) Cyclic voltammetry and XPS studies of electrochemical stability of clean and Pt-modified tungsten and molybdenum carbide (WC and Mo_2C) electrocatalysts. J Power Sources 193:501–506
19. Weigert EC, Humbert MP, Mellinger ZJ, Ren Q, Beebe TP Jr, Bao L, Chen JG (2008) Physical vapor deposition synthesis of tungsten monocarbide (WC) thin films on different carbon substrates. J Vac Sci Tech A 26:23–28
20. Weigert EC, Stottlemyer AL, Zellner MB, Chen JG (2007) Tungsten monocarbide as potential replacement of platinum for methanol electrooxidation. J Phys Chem C 111:14617–14620
21. Weigert EC, Zellner MB, Stottlemyer AL, Chen JG (2007) A combined surface science and electrochemical study of tungsten carbides as anode electrocatalysts. Top Catal 46:349–357

22. Zellner MB, Chen JG (2005) Surface science and electrochemical studies of WC and W_2C PVD films as potential electrocatalysts. Catal Today 99:299–307
23. Weigert EC, Arisetty S, Advani SG, Prasad AK, Chen JG (2008) Electrochemical evaluation of tungsten monocarbide (WC) and platinum-modified WC as alternative DMFC electrocatalysts. J New Mater Electrochem Syst 11:243–251
24. Angelucci C, Deiner L, Nart F (2008) On-line mass spectrometry of the electro-oxidation of methanol in acidic media on tungsten carbide. J Solid State Electrochem 12:1599–1603
25. Ganesan R, Lee JS (2005) Tungsten carbide microspheres as a noble-metal-economic electrocatalyst for methanol oxidation. Angew Chem Int Ed 44:6557–6560
26. Joo JB, Kim JS, Kim P, Yi J (2008) Simple preparation of tungsten carbide supported on carbon for use as a catalyst support in a methanol electro-oxidation. Mater Lett 62:3497–3499
27. Meng H, Shen PK, Wei Z, Jiang SP (2006) Improved performance of direct methanol fuel cells with tungsten carbide promoted Pt/C composite cathode electrocatalyst. Electrochem Solid-State Lett 9:A368–A372
28. Nagai M, Yoshida M, Tominaga H (2007) Tungsten and nickel tungsten carbides as anode electrocatalysts. Electrochim Acta 52:5430–5436
29. Wang ZB, Zuo PJ, Liu BS, Yin GP, Shi PF (2009) Stable PtNiPb/WC catalyst for direct methanol fuel cells. Electrochem Solid-State Lett 12:A13–A15
30. Zhao Z, Fang X, Li Y, Wang Y, Shen PK, Xie F, Zhang X (2009) The origin of the high performance of tungsten carbides/carbon nanotubes supported Pt catalysts for methanol electrooxidation. Electrochem Commun 11:290–293
31. Kelly TG, Stottlemyer AL, Ren H, Chen JG (2011) Comparison of O–H, C–H, and C–O bond scission sequence of methanol on tungsten carbide surfaces modified by Ni, Rh, and Au. J Phys Chem C 115:6644
32. Skoplyak O, Menning CA, Barteau MA, Chen JG (2007) Experimental and theoretical study of reactivity trends for methanol on Co/Pt(111) and Ni/Pt(111) bimetallic surfaces. J Chem Phys 127:114707
33. Chen Z-X, Neyman KM, Lim KH, Rösch N (2004) CH_3O Decomposition on PdZn(111), Pd(111), and Cu(111). A theoretical study. Langmuir 20:8068–8077
34. Jiang RB, Guo WY, Li M, Fu DL, Shan HH (2009) Density functional investigation of methanol dehydrogenation on Pd(111). J Phys Chem C 113:4188–4197
35. Schennach R, Eichler A, Rendulic KD (2003) Adsorption and desorption of methanol on Pd (111) and on a Pd/V surface alloy. J Phys Chem B 107:2552–2558
36. Zhang CJ, Hu P (2001) A first principles study of methanol decomposition on Pd(111): mechanisms for O–H bond scission and C–O bond scission. J Chem Phys 115:7182–7186
37. Greeley J, Mavrikakis M (2002) A first-principles study of methanol decomposition on Pt(111). J Am Chem Soc 124:7193–7201
38. Greeley J, Mavrikakis M (2004) Competitive paths for methanol decomposition on Pt(111). J Am Chem Soc 126:3910–3919
39. Esposito DV, Hunt ST, Stottlemyer AL, Dobson KD, McCandless BE, Birkmire RW, Chen JG (2010) Low-cost hydrogen-evolution catalysts based on monolayer platinum on tungsten monocarbide substrates. Angew Chem Int Ed 49:9859–9862
40. Humbert MP, Menning CA, Chen JG (2010) Replacing bulk Pt in Pt–Ni–Pt bimetallic structures with tungsten monocarbide (WC): Hydrogen adsorption and cyclohexene hydrogenation on Pt–Ni–WC. J Catal 271:132–139
41. Sexton BA (1981) Methanol decomposition on platinum (111). Surf Sci 102:271–281
42. Davis JL, Barteau MA (1987) Decarbonylation and decomposition pathways of alcohols on Pd(111). Surf Sci 187(3):387–406
43. Davis JL, Barteau MA (1990) Spectroscopic identification of alkoxide, aldehyde, and acyl intermediates in alcohol decomposition on Pd(111). Surf Sci 235:235–248
44. Stottlemyer AL, Ren H, Chen JG (2009) Reactions of methanol and ethylene glycol on Ni/Pt: Bridging the materials gap between single crystal and polycrystalline bimetallic surfaces. Surf Sci 603:2630–2638

45. Bozzini B, Gaudenzi GPD, Fanigliulo A, Mele C (2004) Electrochemical oxidation of WC in acidic sulphate solution. Corros Sci 46:453–469
46. El-Aziz AM, Kibler LA (2002) Influence of steps on the electrochemical oxidation of CO adlayers on Pd(111) and on Pd films electrodeposited onto Au(111). J Electroanal Chem 534: 107–114
47. Antolini E (2009) Palladium in fuel cell catalysis. Energy Environ Sci 2:915–931
48. Lee Y-W, Ko A-R, Han S-B, Kim H-S, Kim D-Y, Kim S-J, Park K-W (2010) Cuboctahedral Pd nanoparticles on WC for enhanced methanol electrooxidation in alkaline solution. Chem Commun 46:9241–9243
49. Lu J, Bravo-Suarez JJ, Takahashi A, Haruta M, Oyama ST (2005) In situ UV–vis studies of the effect of particle size on the epoxidation of ethylene and propylene on supported silver catalysts with molecular oxygen. J Catal 232:85–95
50. Singh RN, Singh A, Anindita X (2009) Electrocatalytic activity of binary and ternary composite films of Pd, MWCNT and Ni, Part II: Methanol electrooxidation in 1 M KOH. Int J Hydrogen Energy 34:2052–2057
51. Carrette L, Friedrich KA, Stimming U (2001) Fuel cells—fundamentals and applications. Fuel Cells 1:5–39
52. Cheng X, Peng C, You M, Liu L, Zhang Y, Fan Q (2006) Characterization of catalysts and membrane in DMFC lifetime testing. Electrochim Acta 51:4620–4625
53. Reshetenko TV, Kim H-T, Krewer U, Kweon HJ (2007) The effect of the anode loading and method of MEA fabrication on DMFC performance. Fuel Cells 3:238–245
54. Wee J-H (2006) Which type of fuel cell is more competitive for portable application: direct methanol fuel cells or direct borohydride fuel cells? J Power Sources 161:1–10
55. Bozzini B, Gaudenzi GPD, Busson B, Humbert C, Six C, Gayral A, Tadjeddine A (2010) In situ spectroelectrochemical measurements during the electro-oxidation of ethanol on WC-supported Pt-black, based on sum-frequency generation spectroscopy. J Power Sources 195(13):4119–4123
56. Bozzini B, Gaudenzi GPD, Tadjeddine A (2010) In situ spectroelectrochemical measurements during the electro-oxidation of ethanol on WC-supported Pt-black. Part II: Monitoring of catalyst aging by in situ Fourier transform infrared spectroscopy. J Power Sources 195(24): 7968–7973
57. Esposito DV, Dobson KD, McCandless BE, Birkmire RW, Chen JG (2009) Comparative study of tungsten monocarbide and platinum as counter electrodes in polysulfide-based photoelectrochemical solar cells. J Electrochem Soc 156:B962–B969
58. Esposito DV, Hunt ST, Kimmel YC, Chen JG (2012) A new class of electrocatalysts for hydrogen production from water electrolysis: metal monolayers supported on low-cost transition metal carbides. J Am Chem Soc 134:3025–3033
59. Hsu IJ, Kimmel YC, Jiang XJ, Willis BG, Chen JG (2012) Atomic layer deposition synthesis of platinum–tungsten carbide core–shell catalysts for the hydrogen evolution reaction. Chem Commun 48:1063–1065
60. Hu FP, Shen PK (2007) Ethanol oxidation on hexagonal tungsten carbide single nanocrystal-supported Pd electrocatalyst. J Power Sources 173:877–881
61. Kimmel YC, Esposito DV, Birkmire RW, Chen JG (2012) Effect of surface carbon on the hydrogen evolution reactivity of tungsten carbide (WC) and Pt-modified WC electrocatalysts. Int J Hydrogen Energy 37:3019–3024
62. Falk M, Whalley E (1961) Infrared spectra of methanol and deuterated methanols in gas, liquid, and solid phases. J Chem Phys 34:1554–1568

http://www.springer.com/978-1-4471-4910-1

Electrocatalysis in Fuel Cells
A Non- and Low- Platinum Approach
Shao, M. (Ed.)
2013, XVI, 745 p. 327 illus., 110 illus. in color.,
Hardcover
ISBN: 978-1-4471-4910-1